

Effects of Noise, Correlations and errors in the preparation of initial states in Quantum Simulations

Nayeli Zuniga-Hansen, Yu-Chieh Chi, Mark S. Byrd*
*Physics Department and Computer Science Department,
 Southern Illinois University, Carbondale, Illinois 62901-4401*
 (Dated: May 7, 2022)

In principle a quantum system could be used to simulate another quantum system. The purpose of such a simulation would be to obtain information about problems which cannot be simulated with a classical computer due to the exponential increase of the Hilbert space with the size of the system and which cannot be measured or controlled in an actual experiment. The system will interact with the surrounding environment, with the other particles in the system and be implemented using imperfect controls making it subject to noise. It has been suggested that noise does not need to be controlled to the same extent as it must be for general quantum computing. However the effects of noise in quantum simulations and how to treat them are not completely understood. In this paper we study an existing quantum algorithm for the one-dimensional Fano-Anderson model to be simulated using a liquid-state NMR device. We calculate the evolution of different initial states in the original model, and then we add interacting spins to simulate a more realistic situation. We find that states which are entangled with their environment, and sometimes correlated but not necessarily entangled have an evolution which is described by maps which are not completely positive. We discuss the conditions for this to occur and also the implications.

PACS numbers: 03.65.Yz, 03.67.Ac

I. INTRODUCTION

Simulating quantum systems with quantum systems is one of the primary reasons there is a great deal of interest in building a quantum computing device. The difficulty of simulating quantum systems on a classical computer, mainly due to the exponential increase of the Hilbert space with system size, was Richard P. Feynman's motivation for proposing the idea that a quantum system might perform this task much more efficiently [1]. Lloyd showed later that some quantum systems could be manipulated to represent the evolution of other quantum systems using only local interactions [2].

There are many problems of interest in quantum mechanics which have no known analytical solution. Thus for a wide range of physical systems simulation is a valuable tool for solving quantum mechanical problems. Classical simulation of such systems can quickly become intractable as the number of particles increases. The resources that are required to perform such a task increase exponentially with the size of the system. For example, in order to represent the state of N 2-state particles a 2^N vector is required and for its evolution the unitary will be a $2^N \times 2^N$ matrix [2, 3]. However, only N particles would be necessary to simulate such a system [2, 4]. In this sense, a quantum simulator is conjectured to provide exponential speedup over classical simulation [5]. But that is not the only advantage; other problems such as the sign problem from Quantum Monte Carlo algorithms for fermionic systems, or the exchange-correlation functionals in Density Functional Theory [6, 7] will not be present

in a quantum simulation. Therefore, many difficult problems in particle physics, condensed matter systems, and chemistry, among others, could be tackled [5, 6, 8–20].

Quantum simulations have received a great deal of recent attention since they are feasible without the need for a universal quantum computing device. The question of the universality of Hamiltonians has been addressed to a great extent [21–30] and algorithms have been developed to simulate specific systems [4, 6, 12, 19, 31–40]. In addition, experiments have been designed and implemented [16, 41–47]. However, a great deal of work remains to be done. Currently available quantum simulating devices have relatively few controllable particles. They are, after all, quantum systems that inevitably interact with the surrounding environment and therefore are subject to noise. Just as with quantum computing, this is an important issue when it comes to scalability. It is therefore necessary to study how the interactions affect a quantum simulation.

The purpose of the present work is to study effects of noise in an existing algorithm proposed for a quantum simulation and to take away from this example as much general understanding as we can. The primary noise considered is prior unknown correlations or entanglement within the system and between the simulated system and the environment. We study the evolution of different initial states, including ideal ones and states in which errors are present due to mistakes in preparation and/or interactions with particles in the system and find the dynamical maps that represent the evolution. The algorithm we explore was proposed and developed by Ortiz et al. [6] to simulate the one-dimensional Fano-Anderson model. To examine various behaviors of the system with initial correlations, we first provide a background for the

* mbyrd@siu.edu

quantum simulation in Section I A which focuses on the different sources of noise that can affect the experiments. Section I B provides a brief review of open system quantum dynamics, and discusses dynamical maps and their main characteristics, including requirements for positivity and complete positivity; the purpose is to use dynamical maps to describe general errors in simulations. Section II contains a brief explanation of the algorithm used, including the modifications we made to represent noise in the system. Finally, our results, given in Section IV, are divided in two parts: those states for which the Bloch vector only has a component along the z direction, and those which have some small component along x and a main one along z . We will also discuss why this is important. These two last subsections are subsequently divided into simulations performed with no external noise and simulations with noise. For the purpose of comparison, the parameters of the system were obtained from Ref. [6] and were used for all the considered scenarios.

A. Quantum simulations

There are two classifications of quantum simulators. The Universal Quantum Simulator (UQS) [48] (also referred to as Digital [49]), is a quantum computer represented by the standard circuit model with the set of universal gates that act on a collection of two-state systems [22, 50, 51]. The term *universal* implies that the quantum computer would be able to simulate any arbitrary quantum system [52] which implies universal quantum computation is possible. However, a fully functioning quantum computer has not been built yet. So researchers have designed and implemented devices consisting of smaller and controllable quantum systems specifically intended for simulations. This is the other type of quantum simulators, referred to as Specialized Quantum Simulators (SQS) [48, 55] or analogue quantum simulators [49, 56] since they are not able to be used to simulate any quantum device or computation. Rather, they are able to simulate a smaller, but interesting class of physical systems. Examples of such systems include: ultracold atoms, ion traps, quantum dots, atoms in optical lattices, coupled cavities, photons, electrons floating on He films and NMR devices [4, 16, 18, 19, 32, 42, 43, 47, 49, 53, 54]. In the SQS, universality for all quantum systems is not required, thus many interesting advances and simple simulations have already been performed [16, 18, 38, 41, 42, 44–46, 54, 57–59].

Just as is the case with any other quantum system, unwanted interactions with an environment can have a detrimental effect on the outcome. Error correction and/or prevention is usually required for accurate implementation. However, inaccurate unitary transformations are also a source of noise and the evolution of the system under a specific Hamiltonian is the main problem of interest [3, 60].

All steps, preparation, evolution and measurement,

can cause some error [6, 17] as well as unwanted interactions with other particles in the simulator, etc. It was initially suggested that decoherence in quantum simulations may not need to be treated in the same strict sense as in quantum computation [2] since noise in the simulating system might be able to be identified with noise in the simulated system. The nature of the interactions of the simulator with the bath may not be the same as those of the system of interest and thus error prevention techniques of some sort will almost certainly be required. These include error-correcting codes (QECC) [61–66], decoherence free subspaces/noiseless subsystems (DNS) [67–72] (see also [73, 74] for reviews), and/or dynamical decoupling (DD) [53, 75–85]. However, error correction means an increase in resource requirements, and this can represent a problem with scalability [3, 4, 56, 86, 87] as well as efficiency. In addition, there exist algorithms and observables which have an inherent robustness to errors [88], but this is not the case for all systems and all errors.

It is sometimes, in fact, possible for the errors to be treated quite differently in the simulation of quantum systems. For example, sometimes it is possible to model some of the interactions of an open quantum system, as is done in Refs. [33, 39], in which the bath is simulated as well. Also, Dür et al. propose an algorithm to generate many body interactions [89] to study the influence of noise in the simulation of many body systems. Furthermore, an experimental setup to study open systems is proposed in [18]. In these cases, the environment is included, but external interactions will still be present and will affect the final outcome in an undesirable manner.

Our work examines interactions within the system, where errors in preparation of the initial state give rise to errors. Obviously the initial state is important because the outcome of the simulation depends on it. Also, when errors are caused by initial entanglement, dynamical decoupling cannot remove those errors since these controls rely on local unitary transformations to eliminate Hamiltonian interactions with a bath. Local unitary controls cannot change the entanglement between the system and the bath.

Experimentally, it has been observed that two different state preparation methods may not yield the same result and can have a profound effect on the outcome [90]. We observe the characteristics of the dynamical map, (which will be described more in detail in the next section) that describe the evolution of different initial states and determine their positivity or complete positivity. Until recently, discussions of the evolution of an open quantum system were limited to completely positive maps. However, work by Pechukas [91] and more recently by Shaji and Sudarshan [92] have provided demonstrations that a map does not need to be completely positive for the end result to represent a physical state. In fact, the map does not even need to be positive; it must only be positive on a given domain in order to possibly represent a physical mapping. In certain circumstances dynamical maps can provide information about correlations in the initial

state of the system, which could provide useful information about the effects of noise and interactions in quantum simulations. Furthermore, there are many sets of operators in the operator-sum decomposition which give rise to the same map. This is true of completely positive maps [93, 94] as well as maps which are not completely positive [95].

B. Noise in Quantum Systems, Completely and Non Completely Positive Maps

The density matrix, or density operator, represents our knowledge of the quantum state of a system. In general any density operator must satisfy the following conditions in order to represent a physical state [96]:

$$\rho = \rho^\dagger, \text{ it is Hermitian,} \quad (1)$$

$$\begin{aligned} \rho \geq 0, \text{ it is positive semi-definite,} \\ \text{i.e. its eigenvalues are non-negative,} \end{aligned} \quad (2)$$

$$\begin{aligned} \text{Tr}(\rho) = 1, \text{ it has trace 1,} \\ \text{i.e. the sum of the probabilities is 1.} \end{aligned} \quad (3)$$

The evolution of a closed system is described by a unitary transformation, as

$$\psi(t) = U\psi(0),$$

where $U = \exp iHt$. It follows that

$$\rho(t) = U\rho(0)U^\dagger.$$

The density operator is often written as an expansion of pure states

$$\rho = \sum_j p_j |j\rangle \langle j|,$$

where the p_j are the probabilities associated to each of the states $|j\rangle$. If one of the probabilities is equal to 1 and the rest are 0, then the state is pure. For two-state systems we can write the density operator in terms of the 2×2 unit matrix and the Pauli operators,

$$\rho = \frac{1}{2} (\mathbb{1} + \vec{a} \cdot \vec{\sigma}),$$

where the coefficients a_i are the projections along the x , y and z directions of the so-called Bloch vector. This provides a representation of the quantum state in the well-known Bloch sphere, which is a geometric representation of the states of a qubits in terms of a sphere with radius 1. (For higher dimensional systems, this is referred to as the polarization vector, coherence vector, or generalized block vector. See [97–103] and references therein.). The magnitude of the Bloch vector is constrained by the condition $\sqrt{a_x^2 + a_y^2 + a_z^2} \leq 1$, and $|\vec{a}| = 1$ represents a

pure state. Thus any state on the surface of the Bloch sphere is a pure state. A mixed state is represented by a vector with $|\vec{a}| < 1$. With this notation it is possible to have a visual representation of the quantum states at different times.

A system S that is coupled to an environment E with Hilbert spaces \mathcal{H}_S and \mathcal{H}_E , respectively, can be considered a larger isolated system whose initial state is described by $\rho_{SE}(0)$. The time evolution of this system is then given by the joint evolution of the system and environment [92]

$$\rho_{SE}(t) = U\rho_{SE}(0)U^\dagger.$$

We are often only interested in the evolution of the system, S . Tracing out the environmental degrees of freedom provides us with the reduced dynamics of the system

$$\rho_S(t) = \text{Tr}_E[\rho_{SE}(t)] = \text{Tr}_E[U_{SE}(t)\rho_{SE}(0)U_{SE}^\dagger].$$

With the reduced dynamics of S , we can find the map that transforms the initial state $\rho(0)$, into the final state $\rho(t)$. To obtain the "dynamical map" it is convenient to write the $N \times N$ density operator ρ as a $N^2 \times 1$ column vector that is transformed into another $N^2 \times 1$ column vector through the $N^2 \times N^2$ supermatrix A

$$\rho_{r's'}(t) = A_{r's',rs}\rho_{rs}(0), \quad (4)$$

where A describes the most general evolution of ρ [104]. In matrix notation

$$\rho' = A\rho. \quad (5)$$

Because ρ must be mapped to another positive ρ' the following conditions are imposed on A [96]:

$$A_{r's',rs} = (A_{s'r',sr})^*, \text{ is Hermitian,} \quad (6)$$

$$\sum_{rsr's'} x_r^* x_s A_{rs,r's'} y_{r'}^* y_{s'} \geq 0, A \text{ is positive,} \quad (7)$$

$$\sum_r A_{rr,r's'} = \delta_{r's'}, A \text{ is Trace Preserving.} \quad (8)$$

These conditions ensure the conditions Eqs. (1)-(3) on the density operator are satisfied.

By interchanging indices of A , we obtain another $N^2 \times N^2$ supermatrix B [96]

$$B_{rr',ss'} \equiv A_{rs,r's'}. \quad (9)$$

The $1 \times N^2$ rows of A become the $N \times N$ block matrices of B . The following conditions are imposed on B so that it represents a physical map:

$$B_{rr',ss'} = (B_{r'r,ss'})^*, B \text{ is Hermitian,} \quad (10)$$

$$\sum_{r s r' s'} x_r^* y_{r'} B_{rr', ss'} x_s y_{s'}^* \geq 0, \quad B \text{ is positive semi-definite,} \quad (11)$$

$$\sum_r B_{rr', rs'} = \delta_{r's'}, \quad B \text{ is trace preserving.} \quad (12)$$

From these we may write

$$\rho(t) = B[\rho(0)]. \quad (13)$$

If B is decomposed into its eigenvectors and eigenvalues, the action of the map can be represented as follows

$$B[\rho(0)] = \sum_{\alpha} \lambda_{\alpha} \zeta_{\alpha} \rho(0) \zeta_{\alpha}^{\dagger},$$

where $\lambda_{\alpha} \in \mathbb{R}$ are the eigenvalues. The hermiticity of ρ' is guaranteed by the restriction given in Eq. (10) [104], so that B must be Hermitian. The matrix A is required to transform $\rho(0)$ into another Hermitian state $\rho(t)$, but A is not necessarily Hermitian itself. The complete positivity of the map implies that the final state will be positive. The eigenvalues of B must all be positive for it to be guaranteed to be a completely positive map. If B has a negative eigenvalue but still transforms any positive $\rho(0)$ into a positive $\rho(t)$, then B is a positive but not necessarily completely positive map.

Non-completely positive maps have been measured using quantum process tomography (QPT) [105, 106] which has caused the specifics of QPT to be questioned [107]. But the possibility that a map which is not a completely positive map can transform a valid quantum state into another valid state has brought a great deal of interest in studying the conditions for complete positivity. This is in addition to the interest in it due to the partial transpose as an indicator of entanglement [108, 109].

In 1994, Pechukas showed that complete positivity constrains a system to product states of the form $\rho_{SE} = \rho_S \otimes \rho_E$, where ρ_E is a fixed state of the bath [91, 110] which excludes correlations and does not represent many physical situations. Alicki in Ref. [111] argued that there is no general definition for the reduced quantum dynamics beyond the weak coupling regime, therefore, when the system is in an initially correlated state with the environment, linear assignment maps have no unique definition [107], and linearity would only be preserved for states that are invariant under the transformation [111]. Pechukas replied in Ref. [110], and agreed that open system reduced dynamics can be non-linear. However, Rodriguez-Rosario et al. examine the assignment maps in [107] and argue against giving up linearity by noting that the assignment maps can be linear if the conditions of consistency or positivity are relaxed, and favor relaxing the positivity condition. A quantum system that interacts with the environment before our prescribed $t = 0$ can be described by completely positive dynamics if the environment does not re-act on the system [104], i.e. the coupling is weak and/or the initial state is in a particular form [91].

As mentioned above, when the map is completely positive the eigenvalues of B in Eq. (13) can be taken to all be positive. When they are, Eq. (13) can be rewritten as

$$\rho(t) = B[\rho(0)] = \sum_{\alpha} \lambda_{\alpha} \zeta_{\alpha} \rho(0) \zeta_{\alpha}^{\dagger} = \sum_{\alpha} C_{\alpha} \rho(0) C_{\alpha}^{\dagger}, \quad (14)$$

where $C_{\alpha} = \sqrt{\lambda_{\alpha}} \zeta_{\alpha}$. Eq. (14) is sometimes known as the Kraus representation or operator-sum decomposition [112], although it was originally discussed in this context by Sudarshan, Mathews, and Rau [96]. Jordan, et al. demonstrated that entanglement in the initial state of the system can lead to non-completely positive maps that still transform a positive ρ into another positive ρ [113]. Rodriguez-Rosario, et al. found that for purely classical correlations, the “quantum discord” (defined below) vanishes, and this is a sufficient condition for completely positive reduced dynamics [114]. Later, Shabani and Lidar demonstrated that the quantum discord was also a necessary condition for complete positivity [115]. Quantum discord was introduced by Ollivier and Zurek in 2001, it is defined as a ‘measure of the quantumness of the correlations’ [116], and is calculated as follows:

$$\delta(S : E) = -\text{Tr}(\rho_E \log(\rho_E)) + \text{Tr}(\rho_{SE} \log(\rho_{SE})) - \sum_j \text{Tr}(\Pi_j^E \rho_{SE}) \frac{\Pi_j^E \rho_{SE} \Pi_j^E}{\text{Tr}(\Pi_j^E \rho_{SE})}, \quad (15)$$

where $H(x) = H(\rho_x) = -\text{Tr}(\rho_x \log(\rho_x))$ is the Von Neumann entropy and $-\sum_j \text{Tr}(\Pi_j^E \rho_{SE}) \frac{\Pi_j^E \rho_{SE} \Pi_j^E}{\text{Tr}(\Pi_j^E \rho_{SE})}$ is the conditional entropy, defined as the entropy of the system with respect to a set of projective measurements performed on the environment. Quantum discord provides a measure of the nature of correlations, it vanishes for classical correlations and is maximum when there is entanglement.

II. BACKGROUND

As mentioned before, the extent to which the noise from the environment can be included in a quantum simulation is dependent on both the simulating and simulated systems. Of course it would be useful to have some previous knowledge of the system-bath interactions. However, this is often not the case. Here we study effects of unwanted noise in a quantum simulation using an algorithm [6] that simulates the one dimensional Fano-Anderson model. In this case we have a realistic model of the interaction and use the dynamical maps of the system to describe the noisy evolution. Starting with different initial states of the system and bath, we reduce the dynamics to a two-particle model system. The algorithm requires the two particles to be initialized in a particular state. Due to interactions with external qubits in the simulating device, these initial conditions may be imperfect. In addition, if the particles are allowed to interact for some small time before the beginning of the

actual algorithm, the particles could begin in a correlated or entangled state. We consider the possibility of errors in the preparation of one of the particles in the system as well as the possibility of correlations between particles. We added a visualization of the evolution of the Bloch vector in order to provide an intuitive picture of the differences in the initial states and how they evolve. It is useful to note that, regardless of the non-complete positivity of some of the maps obtained, the final state is a physical state and the system is a realistic physical model with realistic couplings. The significance of these results will be discussed in the conclusions. We now describe our methods and results.

A. Quantum Algorithm

Ortiz, et al. proposed an algorithm for the quantum simulation of the one-dimensional Fano-Anderson model [15]. This model consists of an impurity described by an energy ϵ surrounded by a ring of n spinless fermions having energies ϵ_{k_i} . The fermions interact with the impurity, which is also a spinless fermion, through a hopping potential V [6, 15]. The diagonalized wave-number representation of the Fano-Anderson Hamiltonian is given by [6, 15]

$$H = \sum_{i=0}^n \epsilon_{k_i} c_{k_i}^\dagger c_{k_i} + \epsilon b^\dagger b + V \sum_{i=0}^{n-1} (c_{k_i}^\dagger b + b^\dagger c_{k_i}) \delta_{k_i 0}. \quad (16)$$

The system is mapped via Jordan-Wigner transformation to the spin system to obtain [6]

$$\bar{H} = \frac{\epsilon}{2} \sigma_z^1 + \frac{\epsilon_{k_0}}{2} \sigma_z^2 + \frac{V}{2} (\sigma_x^1 \sigma_x^2 + \sigma_y^1 \sigma_y^2). \quad (17)$$

Ortiz, et al. consider an NMR device for their simulation as do we, but the model is certainly not limited to this type of device. The simulator has an NMR drift Hamiltonian of the form [6]

$$H_d = \frac{1}{2} \left(\frac{(\epsilon + \epsilon_{k_0})}{2} - \sqrt{\left(\frac{(\epsilon - \epsilon_{k_0})}{2} \right)^2 + V^2} \right) \sigma_z^1 + \frac{1}{2} \left(\frac{(\epsilon + \epsilon_{k_0})}{2} + \sqrt{\left(\frac{(\epsilon - \epsilon_{k_0})}{2} \right)^2 + V^2} \right) \sigma_z^2. \quad (18)$$

The control Hamiltonian for spins in the system is

$$H_c(t) = \sum_j [\alpha_{x_j} \sigma_x + \alpha_{y_j} \sigma_y] \sum_{ij} \alpha_{i,j} \sigma_z^i \sigma_z^j, \quad (19)$$

where the α are controllable. The last term is considered controllable because it can be turned on/off with the x and y rotations.

To obtain the representation of the Hamiltonian in Eq. (17), the following control sequence can be applied

to Eq. (18) [6]

$$U = e^{i\frac{\pi}{4}\sigma_x^2} e^{-i\frac{\pi}{4}\sigma_y^1} e^{-i\frac{\theta}{2}\sigma_z^1\sigma_z^2} e^{i\frac{\pi}{4}\sigma_y^1} e^{i\frac{\pi}{4}\sigma_x^1} \times e^{-i\frac{\pi}{4}\sigma_x^2} e^{-i\frac{\pi}{4}\sigma_y^2} e^{i\frac{\theta}{2}\sigma_z^1\sigma_z^2} e^{-i\frac{\pi}{4}\sigma_x^1} e^{i\frac{\pi}{4}\sigma_y^1}. \quad (20)$$

The goal is to see if the initial state of the impurity has changed over time and, if so, how much. For this purpose, we use the time correlation function $C(t) = b(t)b(0)^\dagger$, which in spin operator representation becomes $C(t) = e^{i\bar{H}t} \sigma_-^1 e^{-i\bar{H}t} \sigma_+^1$ [6], where $\sigma_+ = \sigma_x + i\sigma_y$ and $\sigma_- = \sigma_x - i\sigma_y$. The time correlation function provides information about the overlap of the initial and final states of the impurity.

We use the same form of the Hamiltonian in Eq. (17) to perform the unitary evolution on different initial states of the system and perform the same operation regardless of prior interactions. We then obtain the reduced dynamics of the state of the impurity site (qubit 1) and then obtain the dynamical map that describes the evolution. We also calculate the time correlation function for the purpose of comparing the results of the different situations to those of an ideal scenario. In this way we observe the effects of the noise and possible errors in the outcome of the simulation.

B. Simulation with Noise

To include other qubits in the environment surrounding the system of interest we modified the control Hamiltonian in two different ways:

1. First, we added two spins and had them interacting via zz coupling with the particle that represents the state of the fermion site (qubit 2):

$$H_{\text{NMR}} = \frac{1}{2} \left(\frac{(\epsilon + \epsilon_{k_0})}{2} - \sqrt{\left(\frac{(\epsilon - \epsilon_{k_0})}{2} \right)^2 + V^2} \right) \sigma_z^1 + \frac{1}{2} \left(\frac{(\epsilon + \epsilon_{k_0})}{2} + \sqrt{\left(\frac{(\epsilon - \epsilon_{k_0})}{2} \right)^2 + V^2} \right) \sigma_z^2 + \frac{J_{zz}}{4} \sigma_z^2 \sigma_z^3 + \frac{J_{zz}}{4} \sigma_z^2 \sigma_z^4 + \frac{J_{zz}}{4} \sigma_z^3 \sigma_z^4. \quad (21)$$

2. Next, we added an extra particle, which interacts in the same fashion (zz coupling) with both particles that represent the system of interest: the resonant impurity and the fermion site:

$$H_{\text{NMR}} = \frac{1}{2} \left(\frac{(\epsilon + \epsilon_{k_0})}{2} - \sqrt{\left(\frac{(\epsilon - \epsilon_{k_0})}{2} \right)^2 + V^2} \right) \sigma_z^1 + \frac{1}{2} \left(\frac{(\epsilon + \epsilon_{k_0})}{2} + \sqrt{\left(\frac{(\epsilon - \epsilon_{k_0})}{2} \right)^2 + V^2} \right) \sigma_z^2 + \frac{J_{zz}}{4} \sigma_z^1 \sigma_z^3 + \frac{J_{zz}}{4} \sigma_z^2 \sigma_z^3, \quad (22)$$

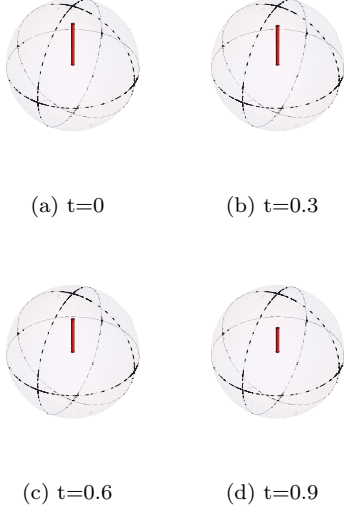


FIG. 1: Evolution of the Bloch Vector of the reduced dynamics of qbit 1 in the initial state $\rho_1 = |0\rangle\langle 0|$ as a function of time.

where J_{zz} represents the zz coupling constant. We used the same control sequence from Eq. (20) to obtain Eq. (17), to represent a situation in which the extra qubits are environmental and thus are taken to be unknown.

III. RESULTS

In this section we describe the results of the simulations for the two different modifications to the Hamiltonian as well as different initial states.

A. States with Bloch vector in the z direction

We first consider states with only a z component to their Bloch vectors. These form a special class of states due to the commutativity of the zz Hamiltonian with these initial states.

1. Noiseless Quantum Simulation

Here we consider the cases where no bath is present, but different initial states are considered. Three cases are considered corresponding to three types of different initial states used in the simulation:

A.1 Pure states

$$|\psi(0)\rangle = |00\rangle, |01\rangle, |10\rangle, |11\rangle. \quad (23)$$

Density operator calculated as $\rho(0) = |\psi(0)\rangle\langle\psi(0)|$.

A.2 Entangled states

$$|\psi(0)\rangle = \alpha_0 |01\rangle + \alpha_1 |10\rangle, \quad (24)$$

where $\alpha_0^2 + \alpha_1^2 = 1$, and the density operator is given by $\rho(0) = |\psi(0)\rangle\langle\psi(0)|$.

A.3 Correlated states

$$\rho(0) = (1-p)(\rho_1^I \otimes \rho_2^I) + p(\rho_1^{II} \otimes \rho_2^{II}), \quad (25)$$

where ρ_1^I and ρ_2^I are the density operators corresponding to some initial state of the impurity (“spin-down”/occupied) and fermion (“spin-up”/unoccupied), respectively, and ρ_1^{II} and ρ_2^{II} correspond to the other initial state of the impurity (“spin-up”/unoccupied) and fermion (“spin-up”/unoccupied).

We represented the initial state of the impurity in terms of its x , y and z projections of the Bloch vector. The magnitude of each component of the projections, a_i , can be obtained by performing the partial trace over everything else except qbit 1, as $a_i = \text{Tr}[\sigma_i(\rho(0))]$.

First consider an initial density operator

$$\rho_S(0) = \frac{1}{2}(\mathbb{1} + \vec{a}_i \cdot \vec{\sigma}_i).$$

In this case, case A.1,

$$\rho_S(0) = \frac{1}{2}(\mathbb{1} + a_3\sigma_z),$$

where a_3 represents a real constant that is equal to, or less than, the radius of the Bloch sphere (i.e. $0 \leq a_3 \leq 1$). It represents the projection along the z axis. The final state was obtained through the reduced dynamics of ρ_S after the evolution:

$$\rho_S(t) = \text{Tr}[\rho_S(0) (U\rho(0)U^\dagger)].$$

When the initial states $\rho_S(0)$ only had a z component, the final states $\rho_S(t)$ only had a z component as well

$$\rho_S(t) = \frac{1}{2}(\mathbb{1} + b_3\sigma_z),$$

where b_3 is another real constant that is subject to $0 \leq b_3 \leq 1$. The value of b_3 depends on a_3 and on the parameters ϵ , ε_{k_i} , V and t . When states with only a z component are input, the final states also only have a z component. This is consistent with the hopping model where the “spin-down” corresponds to the state being occupied. The evolution is described by the dynamical map

$$B = \begin{pmatrix} \frac{1+b_3}{2} & 0 & 0 & 0 \\ 0 & \frac{1+b_3}{2} & 0 & 0 \\ 0 & 0 & \frac{1-b_3}{2} & 0 \\ 0 & 0 & 0 & \frac{1-b_3}{2} \end{pmatrix}. \quad (26)$$

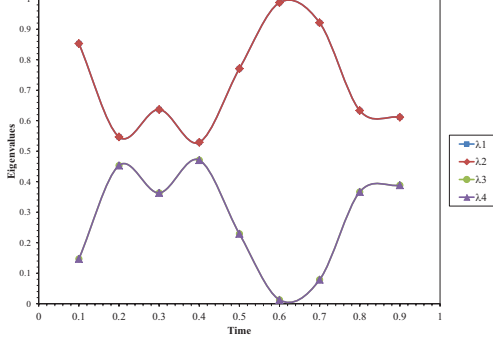


FIG. 2: Eigenvalues of the dynamical map of the reduced dynamics of qbit 1 in the initial state $|\psi\rangle = |01\rangle$ in the closed system. The parameters are $\epsilon = 8$, $\varepsilon = -2$, $V = 4$, for the time interval $\Delta t \in [0.1, 0.9]$.

The the eigenvalues of the map are plotted as functions of time in Figure (2).

The case of a maximally entangled state case A.2 also has a similar form with only a z component. Therefore the map is also given by a form similar to Eq. (26). As can be seen in Fig. (2), the eigenvalues of the map correspond to a completely positive evolution, even though the quantum discord of the initial state was a maximum. Similarly, for case A.3. We therefore note, for later reference, that in these cases all states have only a z component in the initial and final states of the system. Thus there is only this standard interpretation of the hopping model Hamiltonian when there is no external noise.

2. Simulation with noise from spin bath

In this section we present the results for systems governed by the Hamiltonians in Eqs. (21) and (22). The goal is to simulate a two body problem, so we used the same control sequence in Eq. (20). However, the initial state of a “bath” of two particles was included in the total system Hamiltonian. As in the simulation that had no external noise, we chose different initial configurations, Explicitly, including the bath qbits these are:

A.4 Pure states

$$|\psi(0)\rangle = |0011\rangle, |0111\rangle, |1011\rangle, |1111\rangle, \quad (27)$$

and density operator $\rho(0) = |\psi(0)\rangle\langle\psi(0)|$.

A.5 Entangled states

$$|\psi(0)\rangle = \alpha_0 |0111\rangle + \alpha_1 |1011\rangle \quad (28)$$

Where $\alpha_0^2 + \alpha_1^2 = 1$, and the density operator is given by $\rho(0) = |\psi(0)\rangle\langle\psi(0)|$

A.6 Correlated states

$$\rho(0) = ((1-p)(\rho_1^I \otimes \rho_2^I) + p(\rho_1^{II} \otimes \rho_2^{II})) \otimes (|1\rangle\langle 1|) \otimes (|1\rangle\langle 1|). \quad (29)$$

The fact that the states only had a component in the z direction and only interact with the bath via zz couplings resulted in results that were very similar to the ones in the previous section. The initial state of qbit 1 (the impurity) can again be written in Pauli notation as:

$$\rho_S(0) = \text{Tr}_E \rho(0) = \frac{1}{2}(\mathbb{1} + a_3 \sigma_z). \quad (30)$$

The final state is obtained by tracing over the bath degrees of freedom

$$\rho_1(t) = \text{Tr}_E (U\rho(0)U^\dagger) = \frac{1}{2}(\mathbb{1} + b_3 \sigma_z), \quad (31)$$

b_3 is another real constant that can be positive or negative, depending on the direction of the Bloch vector of the final state along the z axis.

The most general dynamical map has the same form as the map in Eq. (26),

$$B = \begin{pmatrix} \frac{1+b_3}{2} & 0 & 0 & 0 \\ 0 & \frac{1+b_3}{2} & 0 & 0 \\ 0 & 0 & \frac{1-b_3}{2} & 0 \\ 0 & 0 & 0 & \frac{1-b_3}{2} \end{pmatrix}. \quad (32)$$

We observed that the coupling J_{zz} has an effect in the rate of change of the state of qbit 1, which is presented in the results for the calculation of the time correlation function. For purposes of comparison, the parameters of the system were the same as the results above. In Figs. (3) and (4), the eigenvalues of B are plotted with the couplings to the particles of the spin bath being $J_{zz} = 8$ and $J_{zz} = \frac{1}{10}$ respectively.

Figs. (2), (3) and (4) show the evolution of the same initial state but each has a different environment. Being states initially in the z direction, the dynamics are completely positive since the interaction with the bath is a zz coupling. However, it does change the hopping rate. In Fig. (3) this is particularly noticeable due to the choice of the coupling. The state of the impurity does not transfer as easily due to the strong correlations generated by the interaction with the spin bath. In Fig. (4) the situation is different. In this case the eigenvalues remained the same regardless of the strength of the coupling with the environment. Having a single extra particle interacting with both qbits with the same strength would mean they both have the same interaction with the bath.

B. Arbitrary initial direction of the Bloch vector

Noise in the initialization of the state could result in a direction for the Bloch vector which is not in the z direction. States that have an x or a y component to their

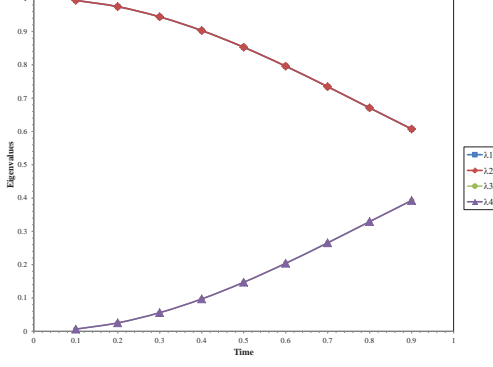


FIG. 3: Eigenvalues of the dynamical map of the reduced dynamics of qbit 1. Two additional qbits are interacting via zz coupling with qbit 2, $J_{zz} = 8$. The initial state of the total system and bath is $|\psi\rangle = |0111\rangle$. The system parameters are $\epsilon = -8$, $\varepsilon = -2$ and $V = 4$, in the time interval $t \in [0.1, 0.9]$.

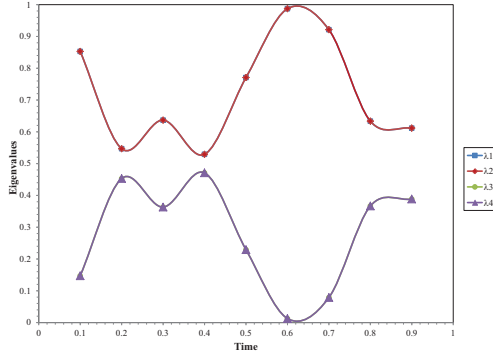


FIG. 4: Eigenvalues of the dynamical map of the reduced dynamics of qbit 1. An additional qbit is interacting via zz coupling with qbits 1 and 2, $J_{zz} = 1/10$. The initial state is $|\psi\rangle = |011\rangle$. The system parameters are $\epsilon = -8$, $\varepsilon = -2$ and $V = 4$, for times $t \in [0.1, 0.9]$.

polarization vector, or Bloch vector, exhibit precession and approximate more accurately what happens in a real experimental situation. In this case, if some initial error on the system has a component in the x or y direction,

Larmor precession will be present. This is often observed in a NMR device under general circumstances and leads to noise in the system. Here we consider an initial state with a component of the Bloch vector in the x direction. Clearly a y component is not necessary, and only specifies a different initial condition for the angle since the system will precess.

1. Noiseless Quantum Simulation

The initial states were chosen to have a component in the x direction; the components in x and z were selected such that the magnitude of the Bloch vector is close to 1 emulating a small error in the initialization. Explicitly, the different initial configurations were:

$$\rho_1(0) = \frac{1}{2}(\mathbb{1} + a_1\sigma_x + a_3\sigma_z),$$

or

$$\rho_2(0) = \frac{1}{2}(\mathbb{1} + a_1\sigma_x - a_3\sigma_z),$$

where ρ_1 is the state of the impurity, ρ_2 is the state of the fermion and the a_i are subject to $0 \leq \sqrt{a_1^2 + a_3^2} \leq 1$. Therefore, the total initial state is

$$\rho(0) = \rho_1(0) \otimes \rho_2(0).$$

The final state of the impurity was, once again, obtained by doing a partial trace over the degrees of freedom of the fermion

$$\rho(t) = \text{Tr}_E(U\rho(0)U^\dagger) = \frac{1}{2}(\mathbb{1} + b_1\sigma_x + b_2\sigma_y + b_3\sigma_z). \quad (33)$$

The map B is given by

$$B = \begin{pmatrix} \frac{1+b_3}{2} & 0 & 0 & \frac{-ib_2}{a_1} \\ 0 & \frac{1+b_3}{2} & \frac{b_1}{a_1} & 0 \\ 0 & \frac{b_1}{a_1} & \frac{1-b_3}{2} & 0 \\ \frac{ib_2}{a_1} & 0 & 0 & \frac{1-b_3}{2} \end{pmatrix}. \quad (34)$$

The eigenvalues of B are given by

$$\lambda_1 = \frac{a_1 - \sqrt{4b_1^2 + a_1^2b_3^2}}{2a_1}, \quad \lambda_2 = \frac{a_1 + \sqrt{4b_1^2 + a_1^2b_3^2}}{2a_1},$$

$$\lambda_3 = \frac{a_1 - \sqrt{4b_2^2 + a_1^2b_3^2}}{2a_1}, \quad \lambda_4 = \frac{a_1 + \sqrt{4b_2^2 + a_1^2b_3^2}}{2a_1} \quad (35)$$

where

$$\begin{aligned}
b_1 &= \left\{ \cos\left(\frac{1}{2}t(\epsilon + \varepsilon_{k_0})\right) \cos\left(\frac{1}{2}t\sqrt{4V^2 + (\epsilon - \varepsilon_{k_0})^2}\right) - \sin\left(\frac{1}{2}t(\epsilon + \varepsilon_{k_0})\right) \left[\frac{(\epsilon - \varepsilon) \sin\left(\frac{1}{2}t\sqrt{4V^2 + (\epsilon - \varepsilon_{k_0})^2}\right)}{\sqrt{4V^2 + (\epsilon - \varepsilon_{k_0})^2}} \right] \right\} a_1, \\
b_2 &= \left\{ -\sin\left(\frac{1}{2}t(\epsilon + \varepsilon_{k_0})\right) \cos\left(\frac{1}{2}t\sqrt{4V^2 + (\epsilon - \varepsilon_{k_0})^2}\right) - \cos\left(\frac{1}{2}t(\epsilon + \varepsilon_{k_0})\right) \left[\frac{(\epsilon - \varepsilon) \sin\left(\frac{1}{2}t\sqrt{4V^2 + (\epsilon - \varepsilon_{k_0})^2}\right)}{\sqrt{4V^2 + (\epsilon - \varepsilon_{k_0})^2}} \right] \right\} a_1 \\
\text{and} \\
b_3 &= \frac{2(-1 + a_3)V^2 + a_3(\epsilon - \varepsilon)^2 + (1 + a_3)V^2 \cos\left(\frac{1}{2}t\sqrt{4V^2 + (\epsilon - \varepsilon)^2}\right)}{4V^2 + (\epsilon - \varepsilon)^2}. \tag{36}
\end{aligned}$$

Note that if $a_1 \mapsto 0$, then b_1 and b_2 are 0. The factor a_1 in the denominator of the eigenvalues is eliminated using l'Hospital's rule, and that yields

$$\begin{aligned}
\lambda_1 &= \frac{1 - b_3}{2}, \quad \lambda_2 = \frac{1 + b_3}{2}, \\
\lambda_3 &= \frac{1 - b_3}{2}, \quad \lambda_4 = \frac{1 + b_3}{2}, \tag{37}
\end{aligned}$$

which are the same as the eigenvalues of the map in Eq. (26). The eigenvalues of B when $a_1 > 0$ are shown in Figure (6). In Fig. (6), the dynamics of the system are positive but not completely positive. This system is not in contact with a bath or reservoir, but it consists of two particles. This is a case of initial correlations between particles in the system, which are errors for this model since correlations should not be present in initial state preparation. The general observation was that when the initial state has a component of the Bloch vector in x or y as well as one in z , the result is a non completely positive map.

2. Simulation with noise from spin bath

The results in this subsection are generated from adding the qubits in the spin bath, and using the following initial states

$$\rho(0) = \rho_1(0) \otimes \rho_2(0) \otimes (|1\rangle\langle 1|) \otimes (|1\rangle\langle 1|), \tag{38}$$

where

$$\rho_1(0) = \frac{1}{2}(\mathbb{1} + a_1\sigma_x + a_3\sigma_z), \tag{39}$$

and

$$\rho_2(0) = \frac{1}{2}(\mathbb{1} + a_1\sigma_x - a_3\sigma_z). \tag{40}$$

The reduced dynamics of S are given by

$$\rho(t) = \text{Tr}_E(U\rho(0)U^\dagger) = \frac{1}{2}(\mathbb{1} + b_1\sigma_x + b_2\sigma_y + b_3\sigma_z), \tag{41}$$

with a B map of the same form as that in Eq. (34),

$$B = \begin{pmatrix} \frac{1+b_3}{2} & 0 & 0 & \frac{-ib_2}{a_1} \\ 0 & \frac{1+b_3}{2} & \frac{b_1}{2} & 0 \\ 0 & \frac{b_1}{a_1} & \frac{1-b_3}{2} & 0 \\ \frac{ib_2}{a_1} & 0 & 0 & \frac{1-b_3}{2} \end{pmatrix}. \tag{42}$$

Once again, the noise, which has the form of purely zz couplings, caused variations in the parameters, mostly in the rate of change of the state of qubit 1. The eigenvalues for a system with two spins interacting with the fermion only and for one spin interacting with both particles in the system are presented in Figs. (7) and (8).

In Figs. (7) and (8) the reduced dynamics are not completely positive. This is due to the initial state of the impurity site (qubit 1) having a component of its Bloch vector in the x direction. The algorithm was designed to have an initial state where one of the two state systems is in the up state and the rest are in the down state. Dynamical maps obtained through quantum process tomography can present discrepancies if the initial states are prepared through different experimental methods [90]. Thus the x component represents a preparation error which gives rise to a non-completely positive map like in the previous case.

C. Time correlation function

Ortiz et al. calculated the time correlation function $C(t) = b(t)b(0)^\dagger$, and plotted the result as $|G|^2 = \text{Tr}(\rho(t)\rho(0))$ as a function of time. Since we want to calculate the effects of noise and different initial state, we followed the same procedure for the different situations. The results are summarized in graphs, Figs. (9), (10) and (11). In Fig. (9), there is a slight difference between the results of the original system compared to those under which errors could arise due to noise and unknown initial states. The coupling to the environment affects how fast or slow qubit 1 evolves. However, if the coupling to the bath is weak, these errors are not as prominent. There was one case in which there was no effect on the speed of change by spins in the bath.

When the initial state had a component in x the resulting correlation functions were very close to the original

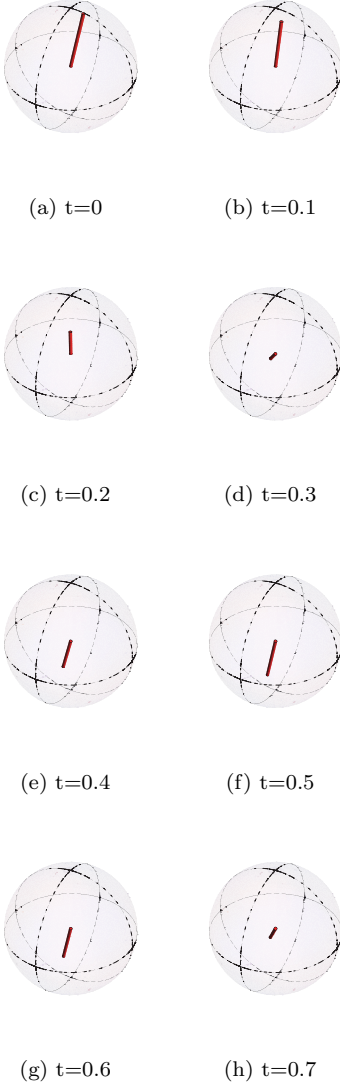


FIG. 5: Animation of the evolution of the Bloch Vector of the reduced dynamics of qbit 1 in the initial state $\rho_1 = \frac{1}{2}(\mathbb{1} + 0.2\sigma_x + 0.97\sigma_z)$

problem. This is important because a small error like this one may not be easily identified in the time correlation function. In Fig. (10) we show how the coupling to a spin bath can affect the rate of change of the evolution. As mentioned before, these results only include zz couplings. The strength of the couplings were adjusted in order to see the effects.

Because quantum simulations are performed on quantum systems, where access to complete information about the state at all times is not available, correlations with the bath can be by detected by differences in the rate of change of the evolution. However, it is useful to also study the case in which the coupling is not only in z . In Fig. (11), we increased a_1 , the component of the Bloch vector in x , to see how it affects the final result. When

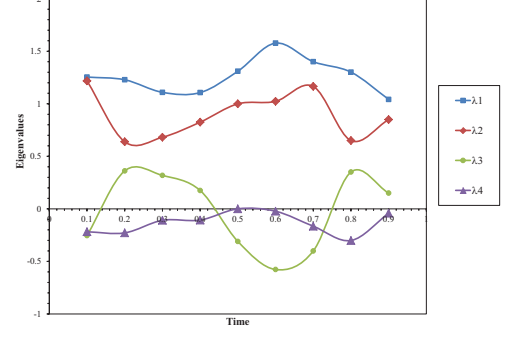


FIG. 6: Eigenvalues for the dynamical map of the reduced dynamics of qbit 1. The initial state of the system is $\rho_1 = \frac{1}{2}(\mathbb{1} + 0.2\sigma_x + 0.97\sigma_z)$, $\rho_2 = \frac{1}{2}(\mathbb{1} - \sigma_z)$. The parameters of the system are $\epsilon = -8$, $\varepsilon = -2$, $V = 4$. Evaluated in the time interval $t \in [0.1, 0.9]$.

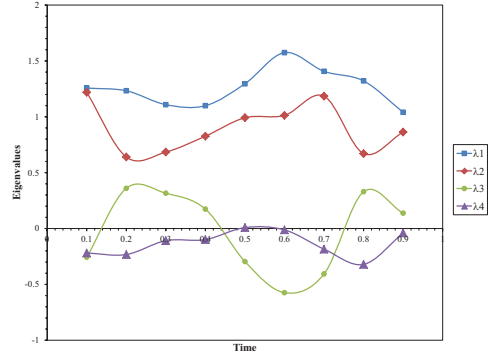


FIG. 7: Eigenvalues of the dynamical map for the reduced dynamics of qbit 1. The initial state of the system is $\rho_1 = \frac{1}{2}(\mathbb{1} + 0.2\sigma_x + 0.97\sigma_z)$, $\rho_2 = \frac{1}{2}(\mathbb{1} - \sigma_z)$, $\rho_3 = \frac{1}{2}(\mathbb{1} - \sigma_z)$, $\rho_4 = \frac{1}{2}(\mathbb{1} - \sigma_z)$. The system parameters are $\epsilon = -8$, $\varepsilon = -2$, $V = 4$, $J_{zz} = \frac{1}{10}$ evaluated in the time interval $t \in [0.1, 0.9]$.

the x component of the Bloch vector is increased, we can see shifts in the time correlation function. The greater a_1 is, the larger the observed shift. This could be useful for detecting possible errors in state preparation.

IV. CONCLUSIONS

Interactions of quantum systems with a surrounding environment are undesirable for reliable quantum simu-

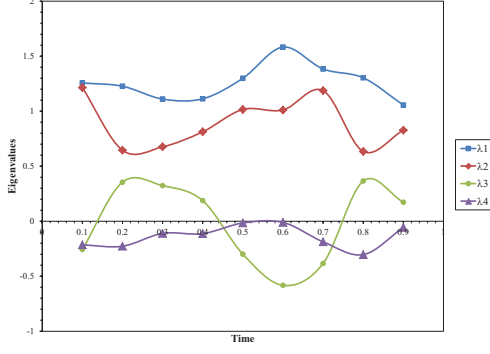


FIG. 8: Eigenvalues of the dynamical map for the reduced dynamics of qbit 1. The initial state of the system is $\rho_1 = \frac{1}{2}(\mathbb{1} + 0.2\sigma_x + 0.97\sigma_z)$, $\rho_2 = \frac{1}{2}(\mathbb{1} - \sigma_z)$, $\rho_3 = \frac{1}{2}(\mathbb{1} - \sigma_z)$. The system parameters are $\epsilon = -8$, $\varepsilon = -2$, $V = 4$, $J_{zz} = \frac{1}{10}$ evaluated in the time interval $t \in [0.1, 0.9]$.

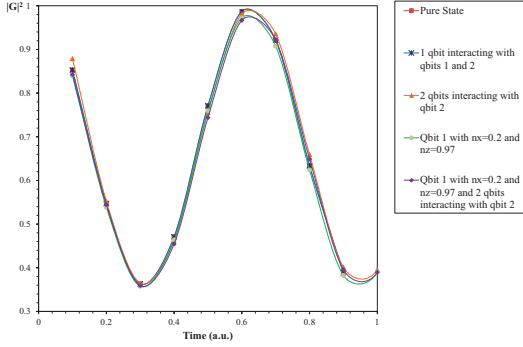


FIG. 9: Time correlation function of the reduced dynamics of qbit 1. The system parameters are $\epsilon = -8$, $\varepsilon = -2$, $V = 4$ and time interval $t \in [0.1, 0.9]$. The results represent the closed system, the system where qbit 2 interacts with two additional qbits, the system in which an additional qbit that interacts with qbits 1 and 2. This was done when qbit 1 was in the initial states $\rho = |0\rangle\langle 0|$ and $\rho = \frac{1}{2}(\mathbb{1} + 0.2\sigma_x + 0.97\sigma_z)$, as indicated above.

lations and for quantum information processing in general. Understanding and controlling or suppressing the noise from the environment is one of the most important objectives of studying open system quantum dynamics. Lloyd's suggestion to use the noise to simulate the interaction of the system with the environment is clearly

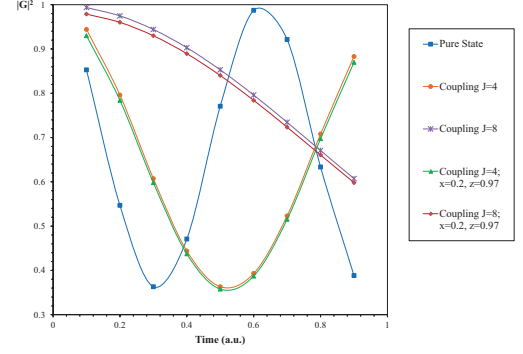


FIG. 10: Time correlation function of the reduced dynamics of qbit 1. The system parameters are $\epsilon = -8$, $\varepsilon = -2$, $V = 4$ in the time interval $t \in [0.1, 0.9]$. The results correspond to the closed system and the system that interacts with two additional qbits, coupled only to qbit 2. The initial state of qbit 1 is $\rho = |0\rangle\langle 0|$ for one set of results, and $\rho = \frac{1}{2}(\mathbb{1} + 0.2\sigma_x + 0.97\sigma_z)$ for the other.

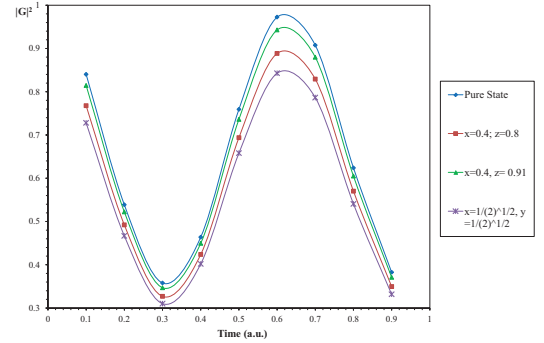


FIG. 11: Time correlation function of the reduced dynamics of qbit 1. The system parameters are $\epsilon = -8$, $\varepsilon = -2$, $V = 4$ evaluated in the time interval $t \in [0.1, 0.9]$. The result represents the time correlation function of the closed system compared to the correlation function of the reduced dynamics of qbit 1 in the initial state $\rho = \frac{1}{2}(\mathbb{1} + a_1\sigma_x + a_3\sigma_z)$ for different values of a_1 and a_3 .

useful only in special cases. For some analog simulators, isolation has nearly been achieved [18], but that will not be the case for many devices. For the cases where noise suppression is required, understanding the noise will be necessary for implementing the appropriate noise control method.

It is known that interactions with the environment can lead to correlations that can result in non completely positive maps. We found that such non completely positive maps are not rare in our study of a very simple model of a quantum system of fermions which can readily be simulated on a quantum computing device, or a dedicated quantum simulator. This Fano-Anderson model exhibits maps which are not completely positive for a variety of initial states, some of which were entangled and some with other non-trivial quantum correlations in the sense of non-zero quantum discord. They were shown to arise for even a fairly small transversal component to an initial density matrix which is supposed to have its Bloch vector aligned along the z axis. Thus fairly small experimental errors can lead to maps which are not completely positive in a rather simple experiment. These noises also cause relatively small errors in the final outcome of the measurement.

Initially correlated states, if they are not so identified,

but are instead identified improperly as arising from completely positive maps, may encourage an experimenter to try to employ dynamical decoupling controls to eliminate errors. These controls will be ineffective in these cases.

We have used a very specific and simple model to illustrate the effects of noise on the system including the presences of maps which are not completely positive. However, it is important to emphasize that these effects are quite general and will be present in some form in many other quantum systems including a wide class of quantum simulations.

ACKNOWLEDGEMENTS

This material is based upon work supported by the National Science Foundation under Grant No. 0545798.

-
- [1] R.P. Feynman, Intl. J. Theor. Phys. **21**, 467 (1982).
 - [2] S. Lloyd, Science **273**, 1073 (1996).
 - [3] K. L. Brown, W. J. Munro and V. M. Kendon, Entropy **12**, 2268 (2010).
 - [4] E. J. Pritchett, C. Benjamin, A. Galiatdinov, M. R. Geller, A. T. Sornborger, P. C. Stancil and J. M. Martinis, (2010), arXiv:1008.0701v1.
 - [5] B.M. Boghosian and W. Taylor, Physica D **120**, 30 (1998).
 - [6] G. Ortiz, J. E. Gubernatis, E. Knill and R. Laflamme, Phys. Rev. A **64**, 022319 (2001).
 - [7] J.D. Biamonte, V. Bergholm, J.D. Whitfield, J. Fitzsimons and A. Aspuru-Guzik, AIP Advances **1**, 022126 (2011).
 - [8] S. Wiesner, "Simulations of Many-Body Quantum Systems by a Quantum Computer," (1996), eprint quant-ph/9603028.
 - [9] C. Zalka, "Efficient Simulation of Quantum Systems by Quantum Computers," (1996), eprint quant-ph/9603026.
 - [10] R. Schack, Phys. Rev. A **57**, 1634 (1998), eprint quant-ph/9705016.
 - [11] S. Somaroo, C. H. Tseng, T. F. Havel, R. Laflamme, and D. G. Cory, Phys. Rev. Lett. **82**, 5381 (1998).
 - [12] I. Kassal, S. P. Jordan, P. J. Love, M. Mohseni and A. Aspuru-Guzik, Proc. Nat. Acad. Sci. USA **105**, 18681 (2008).
 - [13] R. Somma, G. Ortiz, J. E. Gubernatis, E. Knill, and R. Laflamme, Phys. Rev. A **65**, 042323 (2002).
 - [14] R. Somma, G. Ortiz, E. Knill, J. Gubenartis, in *Proceedings of the Society of Photo-Optical Instrumentation Engineers (SPIE)*, Vol. 5105 (2003) p. 96, quant-ph/0304063.
 - [15] C. Negrevergne, R. Somma, G. Ortiz, E. Knill, R. Laflamme, Phys. Rev. A **71**, 032344 (2005).
 - [16] J. Simon, W.S.Bakr, R. Ma, M. E. Tai, P. M. Preiss and M. Greiner, Nature **472** (2011).
 - [17] C. R. Clark, T. S. Metodi, S. D. Gasster and K. R. Brown, Phys. Rev. A **79** (2009).
 - [18] J.T. Barreiro, M. Muller, P. Schindler, D. Nigg, T. Monz, M. Chwalla, M. Hennrich, C. F. Roos, P. Zoller and R. Blatt, Nature **470**, 486 (2011).
 - [19] K. R. Brown, C. Ospelkalus, A. C. Wilson, D. Leibfried and D. J. Wineland, Nature **471**, 196 (2011).
 - [20] S. Bravyi, D. P. DiVincenzo, D. Loss and B. M. Terhal, Phys. Rev. Lett. **101**, 070503 (2008).
 - [21] C.H. Bennett, J.I. Cirac, M.S. Leifer, D. W. Leung, N.Linden, S. Popescu and G. Vidal, Phys. Rev. A **66**, 012305 (2002).
 - [22] Jennifer L. Dodd, Michael A. Nielsen, Michael J. Bremner, Robert T. Thew, (2001), quant-ph/0106064.
 - [23] P. Wocjan, M. Rtteler, D. Janzing, T. Beth, Phys. Rev. A **65**, 042309 (2001).
 - [24] P. Wocjan, M. Roetteler, D. Janzing and T. Beth, Qu. Inf. & Comp. **2**, 133 (2001).
 - [25] P. Wocjan, D. Janzing and T. Beth, Qu. Inf. & Comp. **2**, 117 (2002).
 - [26] M. A. Nielsen, M. J. Bremner, J. L. Dodd, A. M. Childs, C. M. Dawson, Phys. Rev. A **66**, 022317 (2002).
 - [27] M. McKague, M. Mosca and N. Gisin, Phys. Rev. Lett. **102**, 020505 (2009).
 - [28] A. M. Childs, E. Farhi and J. Preskill, Phys. Rev. A **65**, 012322 (2001).
 - [29] A. M. Childs and R. Kothari, Qu. Inf. & Comp. **10**, 669 (2010).
 - [30] A. M. Childs, D. Leung, L. Mancinska and M. Ozols, Qu. Inf. & Comp. **11**, 19 (2011).
 - [31] Wu, L.-A., Byrd, M.S. and Lidar, D.A., Phys. Rev. Lett. **89**, 057904 (2002).
 - [32] S. Mostame and R. Schtzhold1, Phys. Rev. Lett. **101**, 220501 (2008).
 - [33] S. Mostame, P. Rebentrost, D. I. Tsomokos and A. Aspuru-Guzik, (2011), arXiv:1106.1683v1.
 - [34] H. Wang, A. Aspuru-Guzik and M. R. Hoffmann, Phys. Chem. Chem. Phys. **10**, 5388 (2008).
 - [35] J. D. Whitfield, J. Biamonte, A. Aspuru-Guzik, Molecular Physics **109**, 735 (2011).
 - [36] M-H Yung, D. Nagaj, J. D. Whitfield and A. Aspuru-

- Guzik, Phys. Rev. A **82**, 060302 (2010).
- [37] I. Kassal and A. Aspuru-Guzik, J. Chem. Phys. **131**, 224102 (2009).
- [38] B. P. Lanyon, J. D. Whitfield, G. G. Gillett, M. E. Goggin, M. P. Almeida, I. Kassal, J. D. Biamonte, M. Mohseni, B. J. Powell, M. Barbieri, A. Aspuru-Guzik and A. G. White, Nature **2**, 106 (2010).
- [39] H. Wang, S. Ashhab and F. Nori, Phys. Rev. A **83** (2011).
- [40] K. L. Brown, S. De, V. M. Kendon and W. J. Munro, New J. Phys. **13**, 095007 (2011).
- [41] J. Du, N. Xu, X. Peng, P. Wang, S. Wu and D. Lu, Phys. Rev. Lett. **104**, 030502 (2010).
- [42] X.-S. Ma, B. Dakic, W. Naylor and P. Walther, Nature **7**, 399 (2011).
- [43] J. Cho, D. G. Angelakis and S. Bose, Phys. Rev. A **78**, 062338 (2008).
- [44] C. F. Roos, R. Gerritsma, G. Kirchmair, F. Zahringer, E. Solano and R. Blatt, J. Phys.: Conf. Ser. **264**, 012020 (2011).
- [45] R. Gerritsma, G. Kirchmair, F. Zahringer, E. Solano, R. Blatt and C. F. Roos, Nature **463**, 68 (2010).
- [46] R. Gerritsma, B. P. Lanyon, G. Kirchmair, F. Zahringer, C. Hempel, J. Casanova, J. J. Garcia-Ripoll, E. Solano, R. Blatt and C. F. Roos, Phys. Rev. Lett. **106**, 060503 (2011).
- [47] M. Johanning, A. F. Baron and C. Wunderlich, J. of Phys. B **42**, 154009 (2009).
- [48] I. Kassal, J. D. Whitfield, A. Perdomo, M. H. Yung and A. Aspuru-Guzik, Annu. Rev. Phys. Chem. **62**, 185 (2011).
- [49] I. Buluta and F. Nori, Science **326**, 108 (2009).
- [50] D. Deutsch, Proc. Roy. Soc. London Ser. A **400**, 97 (1985).
- [51] V. Pavlov, in *IEEE John Vincent Atanasoff 2006 International Symposium on Modern Computing, Proceedings* (IEEE COMPUTER SOC, 10662 LOS VAQUEROS CIRCLE, PO BOX 3014, LOS ALAMITOS, CA 90720-1264 USA, 2006) p. 235, IEEE John Vincent Atanasoff International Symposium on Modern Computing, Sofia, BULGARIA, OCT 03-06, 2006.
- [52] C.H. Tseng, S. Somaroo, Y. Sharf, E. Knill, R. Laflamme, T.F. Havel, and D.G. Cory, Phys. Rev. A **61**, 012302 (2000).
- [53] D.G. Cory, R. Laflamme, E. Knill, L. Viola, T.F. Havel, N. Boulant, G. Boutis, E. Fortunato, S. Lloyd, R. Martinez, C. Negrevergne, M. Pravia, Y. Sharf, G. Teklemariam, Y.S. Weinstein, W.H. Zurek, Fortschritte der Physik **48**, 875 (2000).
- [54] J. Zhang, G.L. Long, W. Zhang, Z. Deng, W. Liu, Z. Lu, Phys. Rev. A **72**, 012331 (2005).
- [55] M. A. Pravia, Z. Chen, J. Jepe and D. G. Cory, Comp. Phys. Commun. **146**, 339 (2002).
- [56] V. M. Kendon, K. Nemoto and W. J. Munro, The Royal Society A **368**, 3609 (2010).
- [57] E. Jane, G. Vidal, W. Dür, P. Zoller, J.I. Cirac, Qu. Inf. & Comp. **3**, 015 (2003).
- [58] P. Cappellaro, C. Ramanathan, D. G. Cory, Phys. Rev. Lett. **99**, 250506 (2007).
- [59] K. G. H. Vollbrecht and J. I. Cirac, Phys. Rev. A **79**, 042305 (2009).
- [60] D.S. Abrams and S. Lloyd, Phys. Rev. Lett. **79**, 2586 (1997).
- [61] Shor, P.W., Phys. Rev. A **52**, R2493 (1995).
- [62] Steane, A., Rep. Prog. Phys. **61**, 117 (1998).
- [63] Calderbank, A.R. and Shor, P.W., Phys. Rev. A **54**, 1098 (1996).
- [64] Gottesman, D., Phys. Rev. A **54**, 1862 (1996).
- [65] Gottesman, D., *Stabilizer Codes and Quantum Error Correction*, Ph.D. thesis, California Institute of Technology, Pasadena, CA (1997), eprint quant-ph/9705052.
- [66] Gaitan, Frank, *Quantum Error Correction and Fault Tolerant Quantum Computing* (CRC Press, Boca Raton, FL, 2008).
- [67] Zanardi, P. and Rasetti, M., Phys. Rev. Lett. **79**, 3306 (1997).
- [68] Lidar, D.A., Chuang, I.L. and Whaley, K.B., Phys. Rev. Lett. **81**, 2594 (1998).
- [69] Duan, L.-M. and Guo, G.-C., Phys. Rev. A **57**, 737 (1998).
- [70] Knill, E., Laflamme, R. and Viola, L., Phys. Rev. Lett. **84**, 2525 (2000).
- [71] Kempe, J., Bacon, D., Lidar, D.A. and Whaley, K.B., Phys. Rev. A **63**, 042307 (2001).
- [72] Lidar, D.A., Bacon, D., Kempe, J. and Whaley, K.B., Phys. Rev. A **63**, 022306 (2001).
- [73] Lidar, D.A. and K.B. Whaley, in *Irreversible Quantum Dynamics* (Springer-Verlag, Berlin, 2003).
- [74] Byrd, M.S., Wu, L.-A. and Lidar, D.A., J. Mod. Optics **51**, 2449 (2004).
- [75] L. Viola and S. Lloyd, Phys. Rev. A **58**, 2733 (1998).
- [76] Ban, M., J. Mod. Opt. **45**, 2315 (1998).
- [77] L.-M. Duan and G. Guo, Phys. Lett. A **261**, 139 (1999).
- [78] Viola, L., Knill, E. and Lloyd, S., Phys. Rev. Lett. **82**, 2417 (1999).
- [79] Zanardi, P., Phys. Lett. A **258**, 77 (1999).
- [80] D. Vitali and P. Tombesi, Phys. Rev. A **59**, 4178 (1999).
- [81] Viola, L., Lloyd, S. and Knill, E., Phys. Rev. Lett. **83**, 4888 (1999).
- [82] Viola, L., Knill, E., and Lloyd, S., Phys. Rev. Lett. **85**, 3520 (2000).
- [83] D. Vitali and P. Tombesi, Phys. Rev. A **65**, 012305 (2002).
- [84] Byrd, M.S. and Lidar, D.A., Qu. Inf. Proc. **1**, 19 (2001).
- [85] G.S. Agarwal, M.O. Scully and H. Walther, Phys. Rev. Lett. **86**, 4271 (2001).
- [86] K.R. Brown, R.J. Clark and I.L. Chuang, Phys. Rev. Lett. **97**, 050504 (2006).
- [87] A. Papageorgiou and C. Zhang, (2010), arXiv:1005.1318v3.
- [88] Wu, L.-A. and Byrd, M.S., Qu. Inf. Proc. **8** (2009).
- [89] W. Dur, M. J. Bremner and H. J. Briegel, Phys. Rev. A **78**, 052325 (2008).
- [90] A.-M. Kuah, K. Modi, C. A. Rodríguez-Rosario, and E. C. G. Sudarshan, Phys. Rev. A **76**, 042113 (2007).
- [91] P. Pechukas, Phys. Rev. Lett. **73**, 1060 (1994).
- [92] A. Shaji and E.C.G. Sudarshan, Phys. Lett. A **341**, 48 (2005).
- [93] M. A. Nielsen, C. M. Caves, B. Schumacher, H. Barnum, Proc. Roy. Soc. London Ser. A **454**, 277 (1998).
- [94] M. Nielsen and I. Chuang, *Quantum Computation and Quantum Information* (Cambridge University Press, 2000).
- [95] Ou, Y.-C. and Byrd, M.S., Phys. Rev. A **82**, 022325 (2010).
- [96] E. C. G. Sudarshan, P. M. Mathews and J. Rau, Phys. Rev. **121**, 920 (1961).

- [97] Mahler, G. and Weberruss, V.A., *Quantum Networks: Dynamics of Open Nanostructures*, 2nd ed. (Springer Verlag, Berlin, 1998).
- [98] Arvind, K. S. Mallesh and N. Mukunda, J. Phys. A **30**, 2417 (1997).
- [99] B.-G. Englert and N. Metwally, J. Mod. Opt. **47**, 2221 (2000).
- [100] L. Jakóbczyk and M. Siennicki, Phys. Lett. A **286**, 383 (2001).
- [101] Byrd, M.S. and N. Khaneja, Phys. Rev. A **68**, 062322 (2003).
- [102] G. Kimura, Phys. Lett. A **314**, 339 (2003).
- [103] M. S. Byrd, C. A. Bishop, and Y.-C. Ou, Phys. Rev. A **83**, 012301 (2011).
- [104] C. A. Rodriguez-Rosario and E. C. G. Sudarshan, (2008), arXiv:0803.1183v2.
- [105] J. L. O'Brien, G. J. Pride, A. Gilchrist, D. F. V. James, N. K. Langford, T. C. Ralph and A. G. White, Phys. Rev. Lett. **93**, 080502 (2004).
- [106] A. Bendersky, F. Patawski and J. P. Paz, Phys. Rev. Lett. **100**, 190403 (2008).
- [107] C. A. Rodriguez-Rosario, K. Modi, and A. Aspuru-Guzik, Phys. Rev. A **81**, 012313 (2010).
- [108] A. Peres, Phys. Rev. Lett. **77**, 1413 (1996).
- [109] M. Horodecki, P. Horodecki and R. Horodecki, Phys. Lett. A **223**, 1 (1996).
- [110] R. Alicki, Phys. Rev. Lett. **75**, 3020 (1995); P. Pechukas, *ibid.*, p. 3021.
- [111] R. Alicki, Phys. Rev. Lett. **75**, 3020 (1995).
- [112] D. M. Tong, L. C. Kwek, C. H. Oh, Jing-ling Chen and L. Ma, Phys. Rev. A **69**, 054102 (2004).
- [113] T.F. Jordan, A. Shaji and E. C. G. Sudarshan, Phys. Rev. A **70**, 052110 (2004).
- [114] C. A. Rodriguez-Rosario, K. Modi, A.-M. Kuah, A. Shaji and E. C. G. Sudarshan, J. Phys. A **41**, 205301 (2008).
- [115] A. Shabani and D. A. Lidar, Phys. Rev. Lett. **102**, 100402 (2009).
- [116] H. Ollivier and W. H. Zurek, Phys. Rev. Lett. **88**, 017901 (2001).